Comparative Biochemistry and Physiology, Part B 163 (2012) 238–245

Contents lists available at SciVerse ScienceDirect

Comparative Biochemistry and Physiology, Part B

journal homepage: www.elsevier.com/locate/cbpb

Accelerated evolution and functional divergence of scorpion short-chain K^+ channel toxins after speciation

Bin Gao, Shunyi Zhu *

Group of Animal Innate Immunity, State Key Laboratory of Integrated Management of Pest Insects & Rodents, Institute of Zoology, Chinese Academy of Sciences, 1 Beichen West Road, Chaoyang District, 100101 Beijing, China

ARTICLE INFO

Article history:
Received 11 April 2012
Received in revised form 18 June 2012
Accepted 20 June 2012
Available online 26 June 2012

Keywords:
Mesobuthus eupeus
Positive selection
Orthologous gene

ABSTRACT

The α-KTx14 subfamily of scorpion toxins is a group of short-chain polypeptides affecting K^+ channels, including five known members which are restrictedly distributed in *Mesobuthus martensii*. Here, we describe seven new α-KTx14 peptides from *M. martensii* and its sibling species *Mesobuthus eupeus*, two of which (termed MarKTX-3 and MeuKTX-1) were chemically synthesized and refolded for structural and functional studies. Electrophysiological recordings of effects of these two peptides on an array of voltage-gated potassium channels revealed that MarKTX-3 was capable of inhibiting five mammalian K_v1 isoforms ($rK_v1.1$–$rK_v1.5$) and the *Drosophila Shaker* channel with low potency whereas MeuKTX-1 lacks such activity. Circular dichroism spectroscopy analysis combined with homology modeling demonstrates that MarKTX-3 and MeuKTX-1 both adopt a similar cysteine-stabilized α-helical and β-sheet fold. Evolutionary analysis indicates accelerated amino acid substitutions in the mature-peptide-encoding regions of orthologous α-KTx14 peptides after speciation, thereby providing evidences for adaptive evolution and functional divergence of this subfamily.

1. Introduction

Scorpion venom is a rich source of short-chain K^+ channel toxins, which impair the function of a variety of voltage-gated K^+ channels (K_v channels), small-conductance and high-conductance, Ca^{2+}-activated K^+ channels (SK- and BK-channels) (abbreviated as α-KTxs). Based on amino acid sequence similarity, these molecules are categorized into at least 26 different subfamilies (α-KTx1–α-KTx26) (http://www.uniprot.org/docs/scorpktx) (Tytgat et al., 1999; Rodríguez de la Vega and Possani, 2004). Despite extensive sequence divergence, nearly all α-KTxs adopt a conserved cysteine-stabilized α-helical and β-sheet (CSαβ) structural motif, in which a single α-helix spanning CysXaaXaaXaaCys is connected by two disulfide bridges (Cys2/Cys5 and Cys3/Cys6) to the C-terminal β-strand containing CysXaaCys (Xaa, any amino acid), whereas the third disulfide bridge (Cys1/Cys4) links the amino-terminus to the first β-strand (Bontems et al., 1991). One exception was recently reported by Saucedo et al., who found that two new *Tityus*-derived peptides (κ-BUTX-Tt2b and Ts16) with high sequence similarity and identical cysteine spacing to Tt28, a member of α-KTx20, displayed an unconventional disulfide pattern and a complete re-arrangement of the secondary structure topology into a CSαα fold (Saucedo et al., 2012).

K_v channel-targeted α-KTxs have been extensively studied in terms of their structures, functions and action modes. They block the pore of K_v channels by an evolutionarily conserved lysine (Lys) amino-terminal to the fourth cysteine (Lange et al., 2006). In some examples, an aromatic amino acid residue, typically phenylalanine (Phe) or tyrosine (Tyr), constitutes part of a "functional dyad" implicated in channel blockade (Dauplais et al., 1997). The finding of two blockers of K_v channels without the conserved Lys indicates that aside from this documented interaction mode, other modes could exist in these α-KTxs to bind the channel pore (Zhu et al., 2012a,b).

The α-KTx14 subfamily contains five highly similar members (α-14.1 to α-14.5), all derived from *Mesobuthus martensii*. They are composed of 31 residues with three identical disulfide bridges (Rodríguez de la Vega and Possani, 2004). The first members (BmKK1 to BmKK3) were initially identified by screening the venom gland cDNA library (Zeng et al., 2001). Subsequently, the CSαβ structure of BmKK2 (also called BmP07) was confirmed by nuclear magnetic resonance (NMR) (Zhang et al., 2004). In the same year, a new α-KTx14, designated as BmSKTx1, was isolated from the venom and preliminarily identified as a selective inhibitor of apamin-sensitive SK-channels without effect on Na^+, Ca^{2+}, and other types of K^+ channels in DUM neuron (Xu et al., 2004). A large number of polymorphic cDNA and genomic clones were reported in 2005 (Cao et al., 2005).

In this work, we enlarge the α-KTx14 subfamily by adding new cDNA and genomic clones from *M. martensii* and its sibling species *Mesobuthus eupeus*, in which two were chemically synthesized and functionally evaluated against six cloned K^+ channels expressed in *Xenopus* oocytes. By calculating non-synonymous to synonymous nucleotide substitution rate ratios (Yang and Nielsen, 1998), we found

* Corresponding author.
E-mail address: Zhusy@ioz.ac.cn (S. Zhu).

1096-4959/$ – see front matter © 2012 Elsevier Inc. All rights reserved.
doi:10.1016/j.cbpb.2012.06.002

evidence for accelerated evolution between orthologous toxins, which could result in their functional divergence.

2. Materials and methods

2.1. Gene cloning

Total RNAs from 20 venom glands of scorpions (about 10 mg each) were prepared according to the previously described method (Zhu and Gao, 2006) and reverse-transcribed into the first-strand cDNAs using an RT-PreMix kit (SBS Genetech, Beijing) and a universal oligo(dT)-containing adaptor primer (dT3AP), which were directly used as template for PCR by the specific forward primer BmP07L-F (5′-TTTGCTATTCTGCTCATATTG-3′) and 3AP (5′-CTGATCTAGAGGT ACCGGATCC-3′), a universal reverse primer (Zhu and Gao, 2006). BmP07L-F was designed based on the conserved signal peptide-coding regions of the α-KTx14 subfamily. To perform genomic analysis, a reverse primer (BmP07L-R) (5′-CAACTATCATG TACAAGCGCA-3′) was designed to amply genomic DNA in combination with BmP07L-F. PCR products were ligated into the pGEM-T Easy Vector and recombinant plasmids were transformed into *Escherichia coli* DH5a. Positive clones were sequenced with T7 or SP6 primer. Seven cDNA sequences (MeuKTX-1, MeuKTX-2, and MarKTX-1 to MarKTX-5) and four genomic sequences (MeuKTX-1, MarKTX-5, MarKTX-6 and BmKK3) have been deposited in the GenBank database (http://www.ncbi.nlm.nih.gov/) under the accession numbers HQ650826–HQ650832, JQ781064, JQ781065, JQ781066, and JQ798184.

2.2. Chemical synthesis and oxidative refolding

MarKTX-3 and MeuKTX-1 were chemically synthesized in their reduced form by ChinaPeptides Co., Ltd. (Shanghai, China). For oxidative refolding, peptide samples were dissolved in 0.1 M Tris–HCl buffer (pH 8.0) to a final concentration of 1 mM and incubated at 25 °C for 48 h. Peptides were purified to homogeneity by reversed-phase high-pressure liquid chromatography (RP-HPLC). Purity and molecular mass of these peptides were determined by matrix-assisted laser desorption ionization time-of-flight mass spectrometry (MALDI-TOF MS) on a Kratos PC Axima CFR plus (Shimadzu Co. LTD, Kyoto, Japan).

2.3. Circular dichroism spectroscopy

Circular dichroism (CD) spectra of MarKTX-3 and MeuKTX-1 were recorded on a JASCO J-720 spectropolarimeter (Jasco, Tokyo, Japan). Spectra were measured at room temperature by using a quartz cell of 1.0 mm thickness. Data were collected at 0.5 nm intervals with a scan rate of 50 nm/min. CD spectra measurement was performed by averaging three scans. Data are expressed as mean residue molar ellipticity (θ).

2.4. Expression of K_v channels in Xenopus oocytes and two-electrode voltage-clamp recording

For the expression of K_v channels ($rK_v1.1$–$rK_v1.5$ and *Shaker* IR) in *Xenopus* oocytes, the linearized plasmids were transcribed with the T7 mMESSAGE-mMACHINE transcription kit (Ambion, USA) (Table S1). Oocytes were digested for 1–2 h at room temperature in Ca^{2+} free ND96 (in mM: NaCl, 96; KCl, 2; $CaCl_2$, 1.8; $MgCl_2$, 2 and HEPES, 5, adjusted to pH 7.4 with NaOH) containing 0.5 mg/ml collagenase (type I, Sigma). Oocytes were injected with 0.5 ng of cRNA by NANOLITER 2000 (World Precision Instruments Inc., USA). The oocytes were incubated in ND96 solution supplemented with 50 mg/l gentamycin sulfate at 18 °C.

Ion channel currents were recorded 1 to 2 days after injection with Oocyte Clamp OC-725C (Warner Instrument Corp.) and Digidata 1440A (Axon CNS, Molecular Devices) controlled by pClamp10.2 software (Axon Inc., USA). Pipettes were pulled by P-97 Flaming/Brown Micropipette Puller (Sutter Instrument Co., USA) with resistance of 0.1–1.0 MΩ when filled with 3 M KCl. Currents were evoked by 250 ms depolarizations to −10 mV followed by a 250 ms pulse to −50 mV, from a holding potential of −90 mV. All data were recorded from at least 3 independent oocytes ($n \geq 3$) and are presented as mean ± standard error (S.E.). Leak subtraction was carried out with a P/4 protocol. Data was analyzed by pClamp Clampfit 10.0 (Molecular Devices) and SigmaPlot 10.0 (Systat Software, CA, USA).

2.5. Evolutionary analysis

A total of 14 nucleotide sequences of α-KTx14 members, provided in the Supplementary Appendix, were aligned by ClustalX for evolutionary analysis. Non-synonymous to synonymous nucleotide substitution rate ratios ($\omega = dN/dS$) between pairs of genes were calculated by the method of Nei and Gojobori (1986). A neighbor-joining tree (NJ) constructed by MEGA 3.1 (http://www.megasoftware.net) was used for maximum likelihood analysis, in which four models implemented in the CODEML program of the PAML software package (http://abacus.gene.ucl.ac.uk/software/paml.html) were selected to make two likelihood ratio tests (LRTs) by M1a/M2a and M7/M8 (Yang, 2007). Upon detection of positively selected signals, the calculation of posterior probabilities was completed using the Naïve Empirical Bayes (NEB) method under M2a and M8. Sites with a high probability (≥90%) of coming from the class with $\omega > 1$ are likely to be under positive selection.

2.6. Structural modeling of proteins and secondary structure prediction of introns

The experimental structure of BmP07 (PDB entry: 1PVZ) was selected as template to generate MarKTX-3 and MeuKTX-1 models by SWISS-MODEL, a fully automated protein structure homology-modeling server (http://swissmodel.expasy.org/). Model quality was evaluated by Verify3D. Secondary structures of introns were predicted by the MFOLD Web Server in its RNA folding form (http://mfold.rna.albany.edu/).

3. Results

3.1. New members of the α-KTx14 subfamily

Using gene cloning techniques (Fig. 1A), we identified six new α-KTx14 peptides (α-KTx14.6–α-KTx14.11) from *M. martensii*, five encoded by cDNA clones and one by genomic clone, and two new members (α-KTx14.12–α-KTx13) from *M. eupeus* by cDNA cloning. Multiple sequence alignment of the whole subfamily highlights six non-cysteine residues conserved across the alignment, including Thr^{1}, Asp^{12}, Ly^{16}, Gly^{19}, Pro^{21}, and Ala^{29} (Fig. 1B), in which Gly and Pro are defined as structural residues and Asp^{12} and Ly^{16} could form a salt bridge involved in the α-helical stability. All the peptides carry 0.7 to 2.7 of net charges. Peptides derived from the same species are more conserved than those between species, which is supported by a NJ tree where peptides cluster together according to their species origin (Fig. 1C), in favor of independent gene duplication after speciation. Despite closer relationship with the *M. martensii* peptides, MeuKTX-1 and MeuKTX-2 have the same amino-terminal sequence (Thr-Ala-Ile-Ala-Val-Arg-Cys) with BoTx590, an orthologue from *Buthus occitanus* (α-KTx14.14). The latter has a unique carboxyl-terminus ended by Lys-Gly rather than a Thr occurring in all other members. The presence of multiple α-KTx14 isoforms in *M. martensii* is in line with the previous southern hybridization results (Cao et al., 2005).

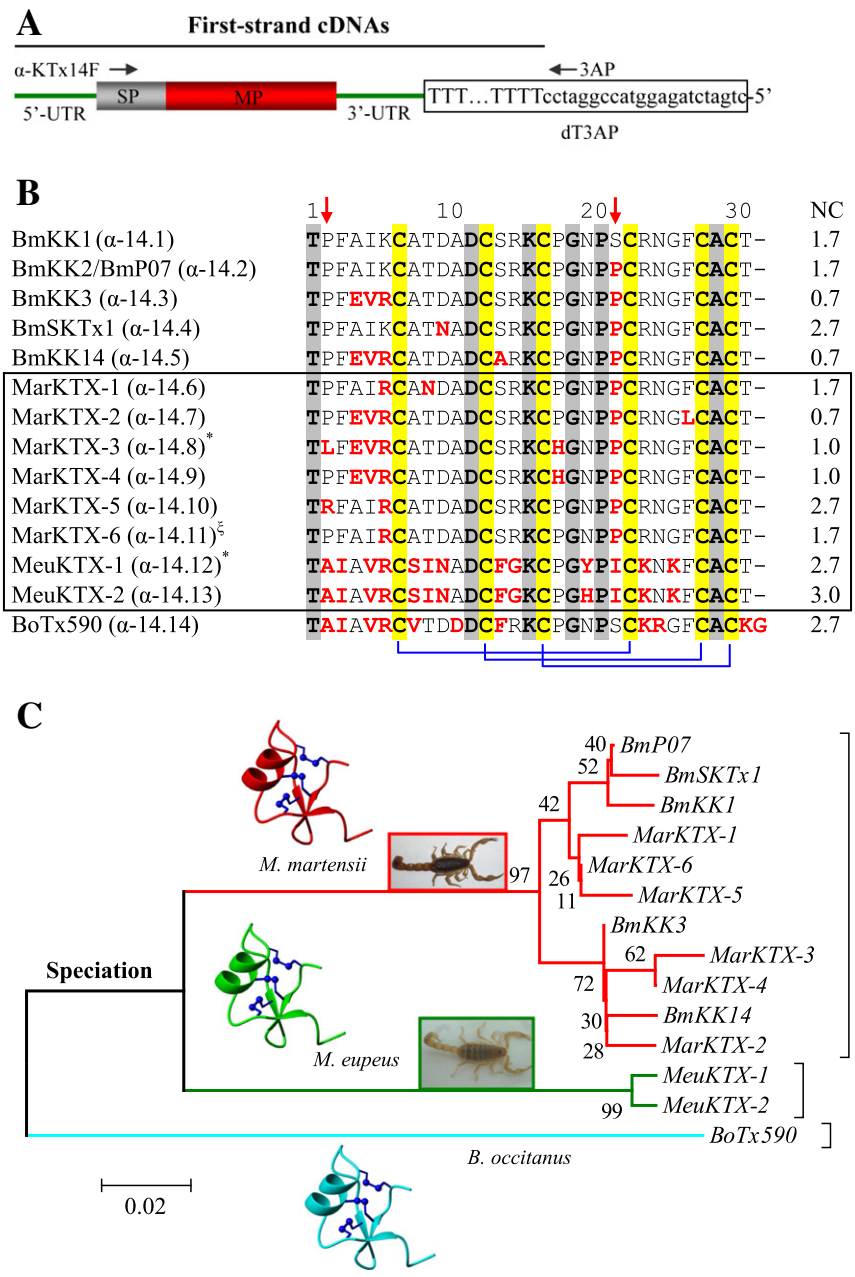

Fig. 1. The α-KTx14 subfamily. A. Schematic showing the first-strand cDNAs reversely transcribed from the venom gland total RNAs of *M. martensii* and *M. eupeus* by dT3AP. Positions of the forward and reverse primers (α-KTx14F and 3AP) are indicated. UTR, untranslated region; SP, signal peptide; MP, mature peptide. B. Multiple sequence alignment showing the amino acid conservation within the subfamily, in which six identical cysteines are shadowed in yellow and other in gray. GenBank accession nos. of previously known sequences: BmKK1 (CAC38035); BmKK2 (CAC38039); BmKK3 (AF325113); BmSKTx1 (AF295594); BmKK14 (AAW62366); BoTx590 (FJ360824). Positively selected sites are shown in red arrows. NC, net charge; *, peptides chosen for synthesis; ξ, the peptide encoded by a genomic clone. C. Neighbor-joining tree, constructed based on the amino acid sequences in (B) by MEGA (http://www.megasoftware.net/), showing clustering of the α-KTx14 subfamily members according to their species origin (*M. martensii*, *M. eupeus* and *B. occitanus*). Nodal support was estimated using the bootstrap approach with 1000 replicates. The scale bar shows total amino acid divergence.

3.2. Comparison of exon and intron sequences

Previous studies have shown that introns are more conserved than their corresponding exons in *M. martensii* α-KTx14 isoforms (Cao et al., 2005). To clarify whether it is the same case for orthologous toxins from the two sibling species of scorpions, we isolated three *M. martensii* genomic DNA clones coding for BmKK3, MarKTX-5 and MarKTX-6, and one *M. eupeus* genomic DNA clone for MeuKTX-1 (Fig. 2A). All the genes contain a phase-1 intron disrupting the Ala codon (GCC) at the end of the signal peptide-encoding region. Remarkably, the introns of the three *M. martensii* genes have completely identical nucleotide sequences while their exons code for different peptide isoforms due to mutations at non-synonymous sites altering their amino acid sequences (Fig. 2B). To uncover putative biological significance of intron conservation between orthologous toxins, we analyzed their RNA secondary structures by MFOLD and found that these introns are able to fold into a similar architecture with two tandem stem-loop structures and 5′- and 3′-splice signals in a proximate distance, which are presumably needed for an efficient intron splicing (Fig. 2C).

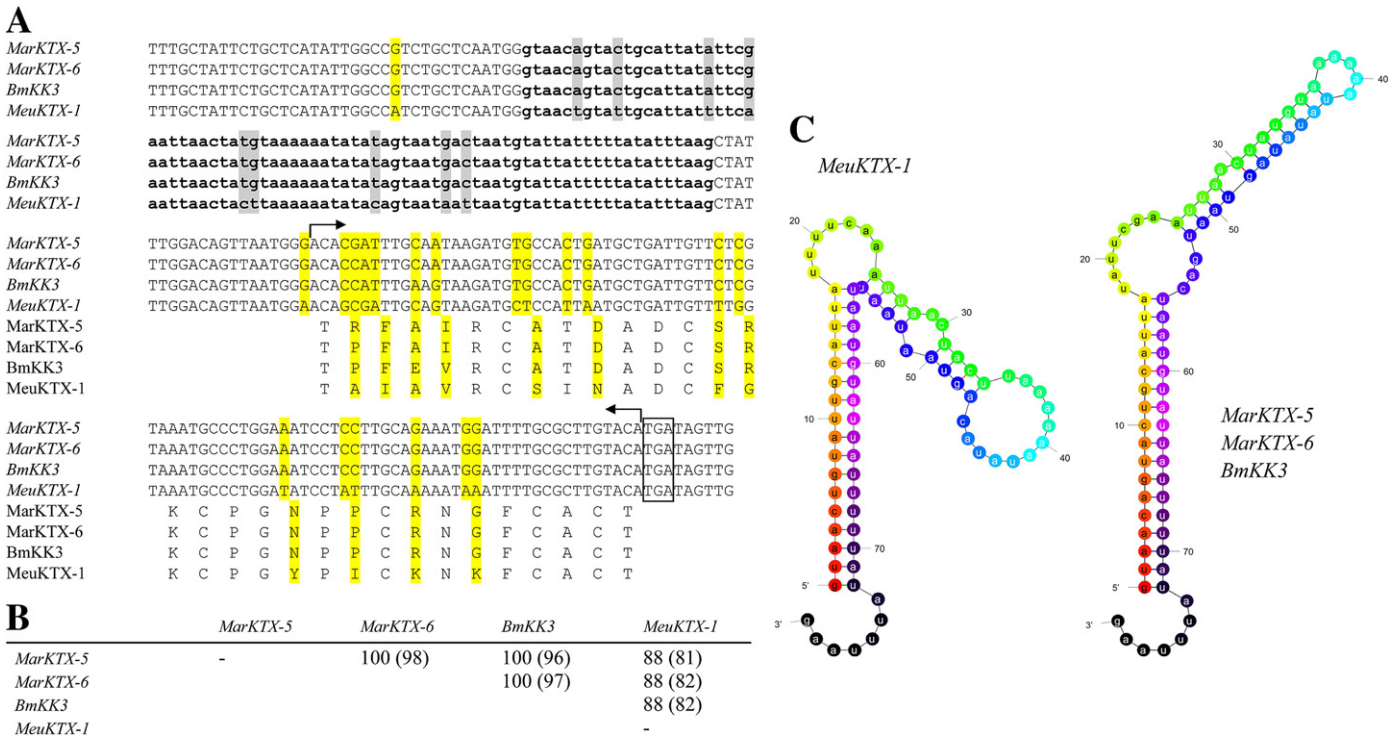

Fig. 2. Comparison of genomic sequences and intron secondary structures of *Mesobuthus* α-KTx14 genes. A. Nucleotide sequence alignment of MarKTX-5, MarKTX-6, BmKK3 and MeuKTX-1. Exon and intron sequences are indicated in uppercase and lowercase letters, respectively. Non-identical sites are shadowed in gray. Arrows label the position of mature peptide-encoding regions. Stop codons are boxed. B. Similarity percentage among nucleotide sequences of introns (exons) among different members. C. Intron secondary structures predicted by MFOLD.

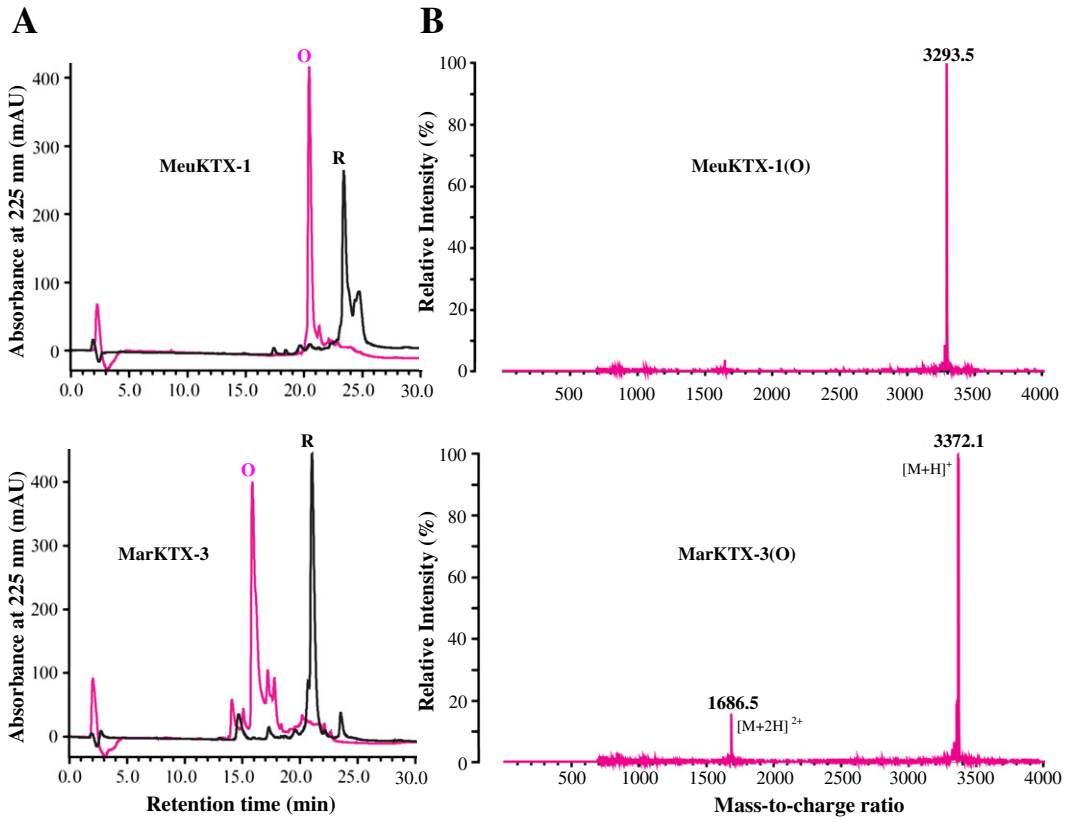

Fig. 3. Oxidative refolding and MALDI-TOF of MeuKTX-1 and MarKTX-3. A. RP-HPLC showing retention time (T_R) difference between the reduced (R) and oxidized (O) peptides. B. MALDI-TOF MS of the oxidized peptides.

3.3. Structural features of MarKTX-3 and MeuKTX-1

MarKTX-3 and MeuKTX-1 were chosen as representatives to study structural and functional features of newly discovered peptides. In RP-HPLC, synthetic reduced peptides were eluted at retention time (T_R) of 23.8 min for MeuKTX-1 and 21 min for MarKTX-3 whereas their corresponding oxidized products were eluted at T_R of 20.5 min and 16 min, respectively (Fig. 3A). Earlier elution for the oxidized peptides may be due to more hydrophobic residues less accessible in a structured molecule when three disulfide bridges were formed. This was verified by MALDI-TOF that gave experimental molecular masses of 3293.5 Da for MeuKTX-1 and 3372.1 Da for MarKTX-3, perfectly matching their calculated molecular masses of 3292.93 Da and 3370.84 Da (Fig. 3B).

Next, we analyzed the secondary structure features of the two synthetic peptides by CD (Fig. 4A). Although overall MeuKTX-1 has a similar CD spectrum to MarKTX-3, their negative minimums are slightly different (213 nm vs. 209 nm). Based on the CD data, we estimated secondary structure contents of these two peptides, which include 26% of α-helix and 39% of β-sheet in MarKTX-3 and 18% of α-helix and 32% of β-sheet in MeuKTX-1 (Fig. 4B). In comparison with MarKTX-3, MeuKTX-1 appears to have a more loosened structure likely due to mutations in secondary structure regions. In BmP07, electrostatic interaction between Asp12 and Arg15 is known to be associated with the α-helical stability (Zhang et al., 2004). However, such interaction is removed due to the mutation (Arg15Gly) in MeuKTX-1. Structural modeling supports that these two peptides can fold into a CSαβ structure. They both have one common electrostatic potential surface (named face A). When the molecules are rotated along the y-axis, face B appears, which contains a large positive charge zone in MeuKTX-1 but a mixture of positive and negative charge zones in MarKTX-3 (Fig. 4C).

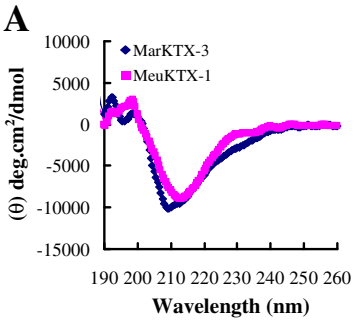

B

Toxin	Secondary structure contents (%)		
	α-helix	β-sheet	Random coil
MarKTX-3	26	39	35
MeuKTX-1	18	32	50

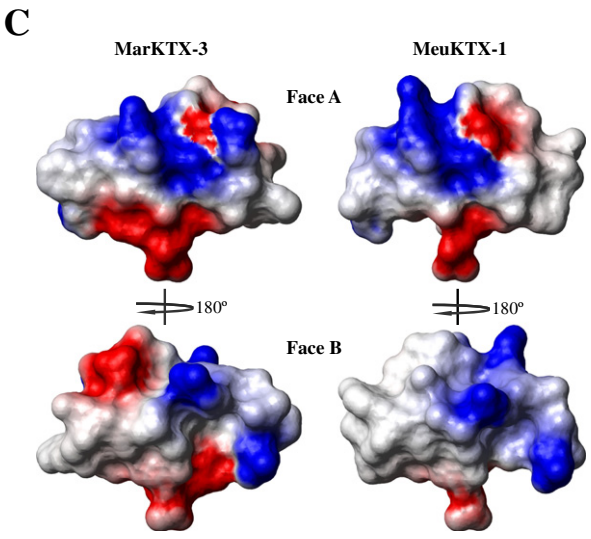

Fig. 4. Structural comparison of MarKTX-3 and MeuKTX-1. A. CD spectra. The spectra were recorded from 190 to 260 nm with a peptide concentration of about 0.3 mg/ml in water. B. Secondary structure contents of MarKTX-3 and MeuKTX-1 estimated from their CD data. C. Electrostatic potential maps of MarKTX-3 and MeuKTX-1 whose structures were built based on the experimental coordinates of BmP07 (PDB entry: 1PVZ).

3.4. Differential pharmacological targets between MarKTX-3 and MeuKTX-1

Electrophysiological recordings of effects of MarKTX-3 and MeuKTX-1 on five rat K_v channel isoforms (rK_v1.1–rK_v1.5) and the *Drosophila Shaker* channel, all expressed in *Xenopus* oocytes, demonstrated that MarKTX-3 had a wide-spectrum of inhibitory activity on all the channels tested with weak potency. At 10 μM concentration, the current percentages of blockade are 23±2.9 (rK_v1.1); 21±12.0 (rK_v1.2); 19±3.7 (rK_v1.3); 38±7.3 (rK_v1.4); 16.7±4.5 (rK_v1.5); and 30.7±4.2 (*Shaker*) (mean±S.E.), respectively (Fig. 5A). By contrast, MeuKTX-1 lacked such activity at the same concentrations (data not shown). Blockade of rK_v1.3 channels occurred rapidly and binding was reversible upon washout (Fig. 5B). Prior investigations have suggested that scorpion toxins could have antimicrobial activity because of the presence of a γ-core motif (Yount and Yeaman, 2004). However, we found that MarKTX-3 and MeuKTX-1 exhibited no antimicrobial activity on an array of microorganisms (data not shown) at high micromolar concentrations.

3.5. Positive selection in Mesobuthus α-KTx14

Positive selection driving adaptive evolution of animal toxins has been observed in many venomous organisms from different phyla (Zhu et al., 2004; Kozminsky-Atias and Zilberberg, 2012; Zhu et al., 2012b). Based on the finding of higher conservation of intron sequences, Cao et al. (2005) proposed adaptive evolution in the *M. martensii* α-KTx14s. However, statistical evidence from the numbers of synonymous and non-synonymous nucleotide substitutions is lacking. The availability of multiple gene sequences provides possibility for statistical analysis of diversifying evolution in this subfamily (Hurst, 2002; Yang, 2007). To test this, we firstly calculated ω (dN/dS) values between pair genes and found that all pairs between paralogous toxins have a ω value of infinity due to the lack of synonymous replacements. Despite this, the presence of non-synonymous replacements in all the pairs of paralogous toxins suggests that adaptive evolution could have taken place after gene duplication. For the orthologous genes between *M. martensii* and *M. eupeus*, all the ω values are >1 (2.2 to 2.6) whereas ω values of the genes between *B. occitanus* and *M. martensii* or *M. eupeus* is <1 (Fig. 6), indicating that accelerated evolution has occurred after divergence of the two sibling species. To identify which sites have been subjected to positive selection, we used maximum-likelihood methods based on models of codon substitution to analyze the data. M2a and M8 models convergently identified two common sites (2 and 22) subjected to positive selection, although comparisons between M2a against M1a and M8 against M7 are not significant ($p=0.34$–0.35) (Table 1). The lack of significance could be due to high sequence similarity resulting in low information content in the data, as observed in protamine P2 and transition protein 2, two female reproductive proteins in mammals (Swanson et al., 2001).

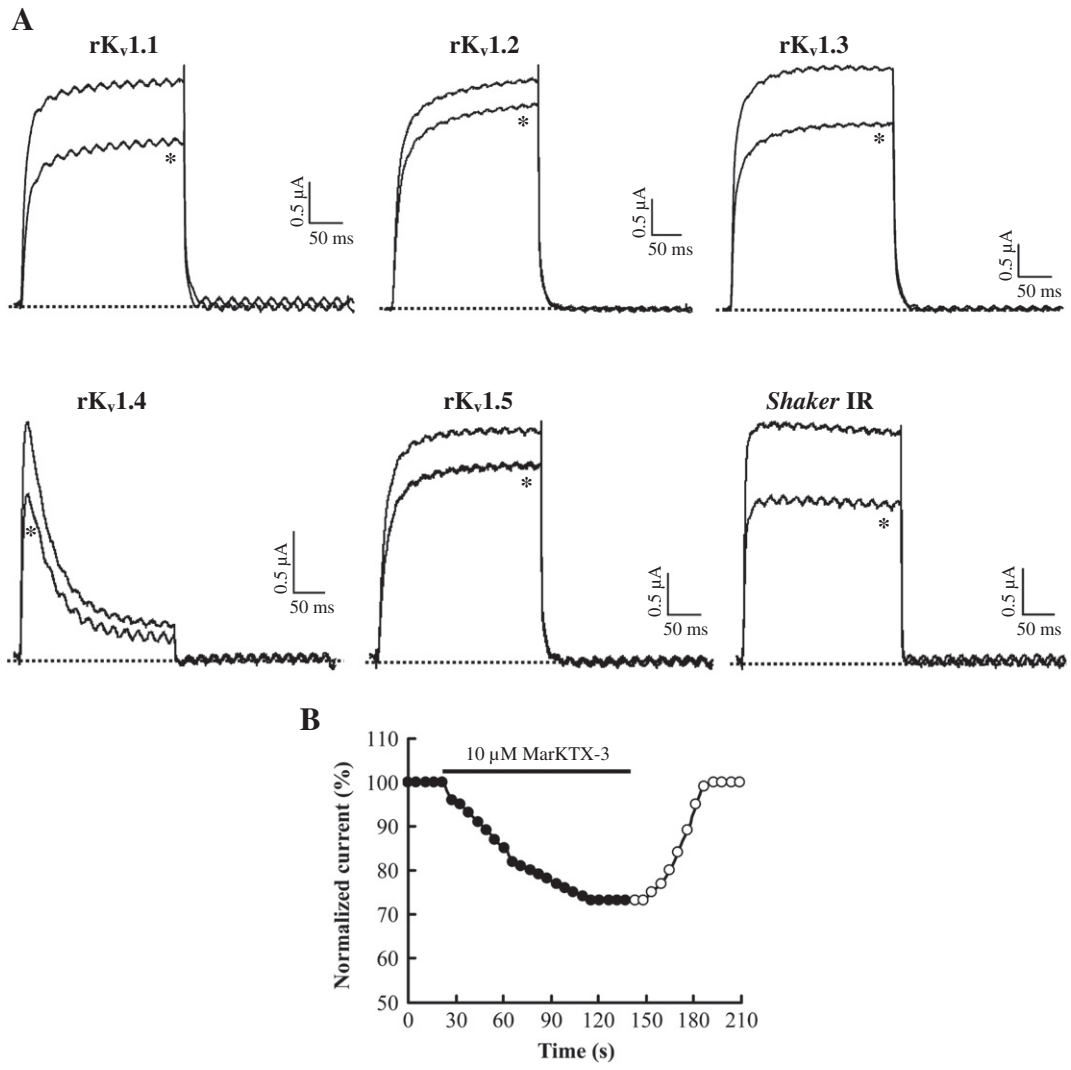

Fig. 5. Inhibitory effect of MarKTX-3 on different K_v channels expressed in *Xenopus* oocytes. A. Representative whole-cell current traces in control and peptide conditions are shown. The dotted line indicates the zero-current level. * indicates steady-state current traces after application of 10μM peptide. Traces shown are representative traces of at least 3 independent experiments (n≥3). B. Reversibility of the inhibition on $rK_v1.1$ upon washout.

	M. eupeus		*M. martensii*										*B. occitanus*
	MeuKTX-1	MeuKTX-2	MarKTX-6	BmP07	BmSKTx1	BmKK1	MarKTX-1	MarKTX-5	MarKTX-3	MarKTX-4	BmKK14	BmKK3	MarKTX-2	BoTx590
MeuKTX-1	-													
MeuKTX-2	∞													
MarKTX-6	2.2729	2.2609												
BmP07	2.4364	2.4235	∞											
BmSKTx1	2.2467	2.2349	∞	∞										
BmKK1	2.4364	2.4235	∞	∞	∞									
MarKTX-1	2.2207	2.2090	∞	∞	∞	∞								
MarKTX-5	2.5001	2.4868	∞	∞	∞	∞	∞							
MarKTX-3	2.6073	2.5935	∞	∞	∞	∞	∞	∞						
MarKTX-4	2.3863	2.3737	∞	∞	∞	∞	∞	∞	∞					
BmKK14	2.4429	2.4299	∞	∞	∞	∞	∞	∞	∞	∞				
BmKK3	2.2527	2.2408	∞	∞	∞	∞	∞	∞	∞	∞	∞			
MarKTX-2	2.5001	2.4868	∞	∞	∞	∞	∞	∞	∞	∞	∞	∞		
BoTx590	0.4975	0.4943	0.2393	0.2597	0.2847	0.2354	0.2555	0.2694	0.3197	0.2879	0.2607	0.2363	0.2694	-

Fig. 6. Pairwise ω estimation of *Mesobuthus* α-KTx14 subfamily members. ω values are shadowed in different colors: <1 (blue); >1 (red); ∞ when dS is 0 (green).

Table 1
Maximum likelihood estimates of parameters for the α-KTx14 family.

Model	S	p	l	κ	Estimates of parameters	PSSs
M0 (one-ratio)	1.53	1	−314.50	2.99	ω=0.68	None
M1a (neutral)	1.59	2	−314.30	2.99	p_0=0.55 (p_1=0.45) ω_0=0.36 (ω_1=1)	Not allowed
M2a (selection)	1.85	4	−313.28	3.06	p_0=0.92 p_1=0.00 (p_2=0.18) ω_0=0.54 (ω_1=1) ω_2=4.47	2, 22
M7 (beta)	1.58	2	−314.37	2.99	p=0.83, q=0.40	Not allowed
M8 (beta and ω)	1.85	4	−313.28	3.06	p_0=0.92 (p_1=0.08) p=99.00, q=82.94 p=99.00, q=82.94	2, 22

Note—S represents tree length; p is the number of parameters in the ω distribution; l is the log likelihood; κ is transition/transversion rate ratio. Twice the log likelihood difference (2Δl) between null models (M1a and M7) and their alternative models (M2a and M8): M1a/M2a=2.04 (χ^2 value: p=0.35); M7/M8=2.18 (p=0.34). PSSs (positively selected sites) were identified by the Naive Empirical Bayes (NEB) methods under M2a and M8.

4. Discussion

It is known that most orthologous genes retain similar function whereas paralogous genes undergo functional diversification (Koonin, 2005). However, some peptide toxins alter their functions after speciation by accelerated evolution. *M. martensii* and *M. eupeus* are two sibling species of scorpions with different geographical distributions in China (Shi et al., 2007). Currently, orthologous relationship of several α-KTxs from these two species has been well established and their structural and functional diversification was also investigated. Such examples include BmP01 and MeuTXKα1; BmTx3B and MeuTx3B (Gao et al., 2011; Zhu et al., 2011). Intriguingly, when compared with MeuTx3B, a weak K_v1.3 blocker, BmTx3B has evolved full blocking capabilities of large conductance calcium-activated K^+ channels (BK) at a concentration of 3 μM. Similarly, it is MarKTX-3 that retained only weak blocking capability of a panel of K_v channels. In these two examples, toxins from *M. martensii* are more potent relative to their *M. eupeus* orthologues (Gao et al., 2011; Zhu et al., 2011), suggesting a possible role of these toxins in ecological adaptation of scorpions if we consider that the former has wider geographical distribution than the latter. A combination of approaches that integrate biochemistry, molecular biology and comparative physiology will help uncover the ecological importance of scorpion toxins, in which *M. martensii* and *M. eupeus* could represent particularly ideal models because of the availability of their toxin information (Goudet et al., 2002; Gao et al., 2011; Zhu et al., 2011).

Recently, accumulated evidence provides more support for functional importance of positively selected sites (PSSs) (Zhu et al., 2004; Kozminsky-Atias and Zilberberg, 2012; Zhu et al., 2012b), in which many were found to be directly involved in interaction with their targets. For MarKTX-3 and MeuKTX-1, the amino acids of the two PSSs are Leu2Ala and Pro22Ile. Accelerated substitution at site 22 could be of particular interest in that a functional Lys directly protruding into the channel pore occupies this position in other α-KTxs with high channel blocking potency. The mutations at this site could thus affect the activity of MarKTX-3 and MeuKTX-1 on K_v channels.

Studies have shown that scorpion venom components with weak blocking activity can enhance the effect of other active neurotoxins (Cohen et al., 2006). Several weak components have been isolated from scorpion venom, such as κ-BUTX-Tt2b and κ-hefutoxin 1, which all block at high micromolar concentrations (Srinivasan et al., 2002; Saucedo et al., 2012). Considering the wide spectrum of channel targets, it is possible that MarKTX-3 acts as an enhancer of other potent α-KTxs. However, targeting other types of channels cannot be completely excluded because of rapid evolution in the mature peptide-coding region of these genes.

Acknowledgments

This work was supported by the National Natural Science Foundation of China (30730015 and 30921006) and the National Basic Research Program of China (2010CB945300).

Appendix A. Supplementary data

Supplementary data to this article can be found online at http://dx.doi.org/10.1016/j.cbpb.2012.06.002.

References

Bontems, F., Roumestand, C., Gilquin, B., Ménez, A., Toma, F., 1991. Refined structure of charybdotoxin: common motifs in scorpion toxins and insect defensins. Science 254, 1521–1523.
Cao, Z., Mao, X., Xu, X., Sheng, J., Dai, C., Wu, Y., Luo, F., Sha, Y., Jiang, D., Li, W., 2005. Adaptive evolution after gene duplication in α-KTx 14 subfamily from *Buthus martensii* Karsch. IUBMB Life 57, 513–521.
Cohen, L., Lipstein, N., Gordon, D., 2006. Allosteric interactions between scorpion toxin receptor sites on voltage-gated Na channels imply a novel role for weakly active components in arthropod venom. FASEB J. 20, 1933–1935.
Dauplais, M., Lecoq, A., Song, J., Cotton, J., Jamin, N., Gilquin, B., Roumestand, C., Vita, C., de Medeiros, C.L., Rowan, E.G., Harvey, A.L., Ménez, A., 1997. On the convergent evolution of animal toxins. Conservation of a diad of functional residues in potassium channel-blocking toxins with unrelated structures. J. Biol. Chem. 272, 4302–4309.
Gao, B., Peigneur, S., Dalziel, J., Tytgat, J., Zhu, S., 2011. Molecular divergence of two orthologous scorpion toxins affecting potassium channels. Comp. Biochem. Physiol. A 159, 313–321.
Goudet, C., Chi, C.W., Tytgat, J., 2002. An overview of toxins and genes from the venom of the Asian scorpion *Buthus martensi* Karsch. Toxicon 40, 1239–1258.
Hurst, L.D., 2002. The Ka/Ks ratio: diagnosing the form of sequence evolution. Trends Genet. 18, 486.
Koonin, E.V., 2005. Orthologs, paralogs, and evolutionary genomics. Annu. Rev. Genet. 39, 309–338.
Kozminsky-Atias, A., Zilberberg, N., 2012. Molding the business end of neurotoxins by diversifying evolution. FASEB J. 26, 576–586.
Lange, A., Giller, K., Hornig, S., Martin-Eauclaire, M.F., Pongs, O., Becker, S., Baldus, M., 2006. Toxin-induced conformational changes in a potassium channel revealed by solid-state NMR. Nature 440, 959–962.
Nei, M., Gojobori, T., 1986. Simple methods for estimating the numbers of synonymous and nonsynonymous nucleotide substitutions. Mol. Biol. Evol. 3, 418–426.
Rodríguez de la Vega, R.C., Possani, L.D., 2004. Current views on scorpion toxins specific for K^+-channels. Toxicon 43, 865–875.
Saucedo, A.L., Flores-Solis, D., Rodriguez de la Vega, R.C., Ramirez-Cordero, B., Hernandez-Lopez, R., Cano-Sanchez, P., Noriega-Navarro, R., Garcia-Valdes, J., Coronas-Valderrama, F., de Roodt, A., Brieba, L.G., Possani, L.D., Del Rio-Portilla, F., 2012. New tricks of an old pattern: structural versatility of scorpion toxins with common cysteine spacing. J. Biol. Chem. 287, 12321–12330.
Shi, C.M., Huang, Z.S., Wang, L., He, L.J., Hua, Y.P., Leng, L., Zhang, D.X., 2007. Geographical distribution of two species of *Mesobuthus* (Scorpiones: Buthidae) in China: insights from systematic field survey and predictive models. J. Arachnol. 35, 215–226.
Srinivasan, K.N., Sivaraja, V., Huys, I., Sasaki, T., Cheng, B., Kumar, T.K., Sato, K., Tytgat, J., Yu, C., San, B.C., Ranganathan, S., Bowie, H.J., Kini, R.M., Gopalakrishnakone, P., 2002. κ-Hefutoxin1, a novel toxin from the scorpion *Heterometrus fulvipes* with unique structure and function. Importance of the functional diad in potassium channel selectivity. J. Biol. Chem. 277, 30040–30047.
Swanson, W.J., Yang, Z., Wolfner, M.F., Aquadro, C.F., 2001. Positive Darwinian selection drives the evolution of several female reproductive proteins in mammals. Proc. Natl. Acad. Sci. U. S. A. 98, 2509–25014.
Tytgat, J., Chandy, K.G., Garcia, M.L., Gutman, G.A., Martin-Eauclaire, M.-F., van der Walt, J.J., Possani, L.D., 1999. A unified nomenclature for short-chain peptides isolated from scorpion venoms: α-KTx molecular subfamilies. Trends Pharmacol. Sci. 20, 444–447.
Xu, C.Q., He, L.L., Brône, B., Martin-Eauclaire, M.F., Van Kerkhove, E., Zhou, Z., Chi, C.W., 2004. A novel scorpion toxin blocking small conductance Ca^{2+} activated K^+ channel. Toxicon 43, 961–971.
Yang, Z., 2007. PAML 4: phylogenetic analysis by maximum likelihood. Mol. Biol. Evol. 24, 1586–1591.
Yang, Z., Nielsen, R., 1998. Synonymous and nonsynonymous rate variation in nuclear genes of mammals. J. Mol. Evol. 46, 409–418.
Yount, N.Y., Yeaman, M.R., 2004. Multidimensional signatures in antimicrobial peptides. Proc. Natl. Acad. Sci. U. S. A. 101, 7363–7368.
Zeng, X., Peng, F., Luo, F., Zhu, S., Liu, H., Li, W., 2001. Molecular cloning and characterization of four scorpion K^+-toxin-like peptides: a new subfamily of venom peptides (α-KTx14) and genomic analysis of a member. Biochimie 83, 883–889.
Zhang, N., Li, M., Chen, X., Wang, Y., Wu, G., Hu, G., Wu, H., 2004. Solution structure of BmKK2, a new potassium channel blocker from the venom of Chinese scorpion *Buthus martensi* Karsch. Proteins 55, 835–845.

Zhu, S., Gao, B., 2006. Molecular characterization of a new scorpion venom lipolysis activating peptide: evidence for disulfide bridge-mediated functional switch of peptides. FEBS Lett. 580, 6825–6836.
Zhu, S., Bosmans, F., Tytgat, J., 2004. Adaptive evolution of scorpion sodium channel toxins. J. Mol. Evol. 58, 145–153.
Zhu, S., Peigneur, S., Gao, B., Luo, L., Jin, D., Zhao, Y., Tytgat, J., 2011. Molecular diversity and functional evolution of scorpion potassium channel toxins. Mol. Cell. Proteomics. http://dx.doi.org/10.1074/mcp.M110.002832-1-11.
Zhu, L., Gao, B., Luo, L., Zhu, S., 2012a. Two dyad-free *Shaker*-type K channel blockers from scorpion venom. Toxicon 59, 402–407.
Zhu, S., Peigneur, S., Gao, B., Lu, X., Cao, C., Tytgat, J., 2012b. Evolutionary diversification of *Mesobuthus* α-scorpion toxins affecting sodium channels. Mol. Cell. Proteomics. http://dx.doi.org/10.1074/mcp.M111.012054-1-18.